Published in final edited form as:
Kidney Int. 2011 October ; 80(7): 719–730. doi:10.1038/ki.2011.122.

The Inducible Deletion of Drosha and MicroRNAs In Mature Podocytes Results In A Collapsing Glomerulopathy

Olga Zhdanova[1,2], **Shekhar Srivastava**[1,3], **Lie Di**[1,3], **Zhai Li**[1], **Leila Tchelebi**[1], **Sara Dworkin**[1], **Duncan B Johnstone**[7], **Jiri Zavadil**[5,6], **Mark M. Chong**[1,5], **Dan R. Littman**[1,4], **Lawrence B. Holzman**[7], **Laura Barisoni**[4], and **Edward Y. Skolnik**[1,2,3]

[1]The Helen L. and Martin S. Kimmel Center for Biology and Medicine at the Skirball Institute for Biomolecular Medicine, New York University Langone Medical Center, New York, New York 10016

[2]Division of Nephrology, Department of Internal Medicine, New York University Langone Medical Center, New York, New York 10016

[3]Department of Pharmacology, New York University Langone Medical Center, New York, New York 10016

[4]Howard Hughes Medical Institute, New York University Langone Medical Center, New York, New York 10016

[5]Department of Pathology, New York University Langone Medical Center, New York, New York 10016

[6]NYU Cancer Institute and Center for Health Informatics and Bioinformatics, New York University Langone Medical Center, New York, New York 10016

[7]Department of Nephrology, University of Pennsylvania School of Medicine, Philadelphia, PA 19104

[8]The Walter and Eliza Hall Institute of Medical Research, Parkville, Victoria 3052, Australia

Abstract

MiRNAs have been shown to play key roles in both the function and differentiation of a number of different cell types. Drosha and Dicer, two RNAase III enzymes, function in a stepwise manner to generate a mature miRNA. Previous studies have demonstrated that podocyte-specific deletion of Dicer during development results in a collapsing glomerulopathy (CG). However these studies did not address whether miRNAs are required for the normal function of a mature podocytes throughout life. In addition, Dicer has functions other than generation of miRNAs. We now show that a podocyte-specific deletion of Drosha results in a similar phenotype to Dicer mutants confirming that the Dicer mutant phenotype is due to the loss of miRNAs. Moreover, we demonstrate that inducible deletion of Drosha in 2–3 month old mice results in a CG, thereby demonstrating for the first time that miRNAs are required for the normal function of mature podocytes. The finding that loss of miRNAs in mature podocytes leads to a CG is consistent with the idea that changes in specific miRNAs in the various podocytopathies may directly mediate disease, and suggests that identifying these miRNAs will provide new insight into disease pathogenesis and novel therapeutic targets.

Corresponding Author: Edward Skolnik, Edward.Skolnik@nyumc.org, Phone: 212-263-7458, Fax: 212-263-3110.

Disclosure: All the authors declared no competing interests.

Introduction

MiRNAs (miRNAs) are short (~22 nt) noncoding regulatory RNAs in plants and animals that inhibit gene expression by targeting protein-encoding mRNAs for translational repression or degradation.[1, 2] MiRNAs bind to complementary sites within the 3′ untranslated regions of their target mRNAs.[3, 4] The generation of miRNAs starts from transcription of large RNA precursors, termed pri-miRNAs, from the genome by RNA polymerase II or III. Pri-miRNAs are then processed in the nucleus into shorter sequences of approximately 70 nucleotides, termed pre-miRNAs, by the RNase III enzyme Drosha and the protein Pasha complex.[5–7] Pre-miRNAs have imperfect stem-loop structure and are transported into the cytoplasm where the RNase III enzyme, Dicer, and its dsRNA binding partner, TRBP, excise double-stranded miRNAs of approximately 22 nucleotides.[8, 9] The miRNA joins the miRNA-associated multiprotein RNA-induced silencing complex (miRISC).[10] The mature miRNA strand is preferentially retained in the miRISC and guides it to the target sequence.

At present, over 1000 miRNAs have been identified in humans/mammals. Current estimates predict that about 60% of all human genes are regulated by miRNAs,[11] with a single miRNAs capable of binding and regulating more than 200 target sequences. A large number of papers have now described functional roles for miRNAs in a number of biological processes including cell fate and differentiation, development, cell proliferation, and apoptosis.[12–14] It is also evident that miRNAs play critical roles in maintaining normal health and tissue homeostasis, and changes in miRNA expression are highly relevant to disease processes.

Recently, a number of studies have begun to address the role of miRNAs in kidney disease.[15] These studies have demonstrated that a number of miRNAs are expressed in the kidney, and changes in miRNA expression may contribute to disease.[16, 17] Targeted deletion of Dicer in proximal tubule cells has been shown to protect mice from ischemic reperfusion injury.[18] In diabetic nephropathy, TGF-β upregulation of miR-216a and miR-217 in mesangial cells may promote their survival and hypertrophy, while upregulation miR-377 by high glucose may contribute to mesangial cell production of fibronectin,[19] and downregulation of miR192 in proximal tubule cells may contribute to interstitial fibrosis.[19, 20] Changes in miRNA expression patterns may also contribute to hepatic and renal cyst formation in Autosomal Dominant Polycystic Kidney Disease,[21, 22] and may serve as biomarkers for kidney transplant rejection.[23]

In addition to the above studies, three reports have recently shown that miRNAs may also play critical roles in podocyte homeostasis.[24–26] These studies demonstrated that podocyte-specific deletion of Dicer led to podocyte dysregulation resulting in proteinuric renal disease and collapsing glomerulopathy (CG) with glomerular and tubulointerstitial fibrosis and renal failure at about 6–8 weeks of age. However, in addition to playing a critical role in miRNA biogenesis, Dicer also has functions that are independent of miRNA biogenesis. For example, Dicer is also critical for generating small inhibitory RNAs (siRNAs) derived from endogenous or exogenous dsRNA transcripts.[27, 28] Thus, while decreased expression of miRNAs in podocytes lacking Dicer has been implicated in the development of the CG phenotype, it is not known whether this phenotype is due solely to the loss of miRNAs, or whether miRNA independent functions of Dicer contribute to the phenotype. Moreover, since Dicer is deleted in developing kidneys in these studies, it still remains to determine whether the inducible deletion of dicer in a fully developed kidney also results in a similar phenotype.

To address whether the phenotype in podocyte-specific Dicer knockouts is due solely to miRNA-dependent regulation of normal podocyte function, or whether other functions of Dicer contribute to the phenotype observed, we generated mice in which Drosha was specifically deleted in podocytes. We found that specifically inactivating Drosha in podocytes led to CG that was comparable to the podocyte-specific Dicer knockouts previously described. In addition, we found that inducibly deleting Drosha in podocytes at 2 months of age also led to a CG. Thus, these findings reinforce the critical role for miRNAs in normal podocyte biology and suggest that identifying changes in miRNA expression in various podocyte diseases may provide novel therapeutic targets to treat disease.

Results

Podocyte-specific deletion of Drosha results in collapsing glomerulopathy that is comparable to Dicer KOs

Drosha$^{fl/fl}$ mice have been previously described[29] in which exon 9 is flanked by loxP sites. Deletion of exon 9 disrupts both the full length Drosha as well as 2 alternately spliced forms and results in a frame shift and the appearance of multiple stop codons. Podocyte-specific Drosha knockout mice were generated by breeding *Drosha*$^{fl/fl}$ to *NPHS2-Cre; Drosha*$^{fl/+}$ (NPHS2-Cre mice were provided by L. Holzman, University of Michigan). *Dicer*$^{fl/fl}$ mice were provided by M. McManus and have been previously described.[30] Podocyte-specific Dicer knockouts were generated by crossing *Dicer*$^{fl/fl}$ to *NPHS2-Cre; Dicer*$^{fl/+}$.

NPHS2-Cre; Drosha$^{fl/fl}$ mice were born at the expected Mendelian frequency. However, *NPHS2-Cre; Drosha*$^{fl/fl}$ mice developed proteinuria at about 2–3 weeks of age that progressed overtime with renal failure and death occurring between 4–8 weeks of age (Figure 1 and data not shown). *NPHS2-Cre; Drosha*$^{fl/+}$ mice containing a heterozygous deletion of Drosha in podocytes were phenotypically normal and did not develop proteinuria or histological evidence of kidney disease up until 12 months of age.

Histological examination of *NPHS2-Cre; Drosha*$^{fl/fl}$ mice up until postnatal day 14 revealed normal glomeruli with no apparent abnormality in glomerular development by either light or electron microscopy (data not shown). However, significant glomerular pathology became apparent after postnatal day 14 that progressed over time. At 3 weeks of age, kidneys from *NPHS2-Cre; Drosha*$^{fl/fl}$ mice were smaller and paler when compared with *NPHS2-Cre; Drosha*$^{+/+}$ kidneys. Extensive foot process effacement and mild wrinkling of the glomerular basement membranes on electron microscopy was the earliest pathologic finding and coincided with the onset of proteinuria (figure 2(ii), early). Histopathological examination of *NPHS2-Cre; Drosha*$^{fl/fl}$ kidneys by periodic acid-Schiff-stain (PAS) between 2 and 3 weeks of age revealed only very focal collapsing changes (affecting approximately 10% of the total number of glomeruli), and rare (0.5–1+) cystic dilatation of tubules as well as microcysts, which contained protein casts in the lumen.

At 4–6 weeks age, kidneys from *NPHS2-Cre; Drosha*$^{fl/fl}$ mice demonstrated extensive CG, with extensive segmental and/or global collapse of the glomerular tuft coupled with marked extracapillary proliferation (figure 2(i), Tables 1 and 2). Pseudocrescent formation was found in approximately 45% of glomeruli and segmental or global sclerosis was seen in 28% of the total number of glomeruli, indicating progression of the disease. Simultaneously, the remaining parenchyma was also remarkable for extensive microcyst formation (3+) (figure 2(i), Tables 1 and 2). On ultrastructural analysis, collapsing features were more severe and complete occlusion of the glomerular capillary lumina by severe collapse of the glomerular basement membranes could be appreciated, together with extensive podocyte injury with the loss of primary and secondary foot processes (figure 2(ii), advanced). These changes were proportional to the extent and duration of proteinuria. Similar pathology was found in

kidneys from *NPHS2-Cre; Dicer*$^{fl/fl}$ mice (Tables 1 and 2, Figure 2(i) and 2(ii)), although kidneys from *NPHS2-Cre; Drosha*$^{fl/fl}$ mice exhibited more severe disease at younger age (data not shown).

Deletion of Drosha in podocytes leads to podocyte dedifferentiation and loss of the podocyte-specific markers synaptopodin, WT-1, podocin, and nephrin

CG is associated with podocyte dedifferentiation and loss of podocyte-specific markers. Podocytes from *NPHS2-Cre; Drosha*$^{fl/fl}$ mice exhibited loss of synaptopodin and WT-1, which was first noted at the onset of proteinuria and progressed over time as the kidney disease progressed (figure 3, Table 3). Similar findings were found in kidneys from *NPHS2-Cre; Dicer*$^{fl/fl}$ mice (figure 3, Table 3), with the exception that WT-1 expression was lost at an earlier age in *NPHS2-Cre; Drosha*$^{fl/fl}$ mice, which is consistent with kidneys from *NPHS2-Cre; Drosha*$^{fl/fl}$ mice exhibiting a more severe phenotype at an earlier age (data not shown).

Podocin and nephrin expression were examined by immunofluorescent staining in *NPHS2-Cre; Drosha*$^{fl/fl}$ mice of different ages to further characterize the temporal course of podocyte injury. The glomeruli of *NPHS2-Cre; Drosha*$^{fl/fl}$ mice with minimal changes of CG (age 2 weeks) showed near normal levels of nephrin and podocin expression when compared to wild type animals (Figure 4(i) and 4(ii)) indicating that podocyte development is normal in *NPHS2-Cre; Drosha*$^{fl/fl}$ mice. However, at 5–6 weeks of age when *NPHS2-Cre; Drosha*$^{fl/fl}$ mice have severe CG, levels of both nephrin and podocin were significantly reduced in glomeruli of *NPHS2-Cre; Drosha*$^{fl/fl}$ mice. Nephrin and podocin also displayed a disorganized and granular pattern of distribution in *NPHS2-Cre; Drosha*$^{fl/fl}$ mice that could also be appreciated in glomeruli with early podocyte injury. (Figure 4(i) and 4(ii))

Deletion of Drosha in podocytes leads to increased podocyte proliferation and apoptosis and upregulation of desmin and smooth muscle actin (SMA)

Tissue injury in a number of different cell types is frequently associated with increased expression of intermediate filament (IF) proteins.[31] In podocytes, the IF protein desmin is upregulated in a number of experimental models of podocyte injury.[32–34] Desmin is also upregulated in glomeruli in *NPHS2-Cre; Drosha*$^{fl/fl}$ mice, which is consistent with significant podocyte damage in these mice. Desmin positive cells were primarily localized to proliferating cells (Ki-67 positive) in the urinary space, which were likely podocytes because they also stained for the podocyte-specific marker nestin[35] (figure 5, table 3). Quantification of podocyte proliferation in *NPHS2-Cre; Drosha*$^{fl/fl}$ mice demonstrated an increase in the proliferative index (PI) in epithelial cells in the urinary space (Table 4, PI in *NPHS2-Cre; Drosha*$^{fl/fl}$ mice (4–6 weeks) = 0.656 (range 0.261–0.753); PI in *NPHS2-Cre; Drosha*$^{fl/fl}$ mice (2 weeks) = 0; PI in *NPHS2-Cre; Drosha*$^{+/+}$ mice = 0). In addition, smooth muscle actin (SMA) was also upregulated in glomeruli of *NPHS2-Cre; Drosha*$^{fl/fl}$ mice (figure 5(i)). While early on in disease SMA is most prominently localized periglomerularly (data not shown), in advanced disease cells in the urinary space stained prominently for SMA (figure 5(i)). Podocytes from *NPHS2-Cre; Drosha*$^{fl/fl}$ also exhibited increased apoptosis compared to *wt* animals and the increase in apoptosis increased with time as CG became more advanced (figure 5(ii)).

Conditional inducible deletion of Drosha in podocytes at 2 months of age also results in a collapsing glomerlopathy

In order to determine whether miRNAs are required for the normal function of mature podocytes, a Tet-On system was utilized to specifically delete Drosha in podocytes in 2 month old animals. Drosha$^{fl/fl}$;podocin-rtTA$^{tg/+}$; tetO-Cre$^{Tg/+}$ mice were either administered, or not administered doxycycline at 2 months of age and kidneys were

analyzed 1 month later. Previous studies have demonstrated specific deletion of the gene of interest in 80% of podocytes in these mice using a Z/EG reporter[36]. We have also confirmed specific deletion of exon 9 of the Drosha gene in glomeruli isolated only from mice given doxycycline (figure 6(i)). As expected, kidneys sections were normal in animals not exposed to doxycycline (figure 6 (iii) A,C), and these mice did not develop proteinuria (6ii). In contrast, Drosha$^{fl/fl}$;podocin-rtTA$^{tg/+}$; tetO-Cre$^{Tg/+}$ mice administered doxycycline developed proteinuria begining about 2 weeks after starting doxycycline (figure 6(ii)), which on histological examination revealed a phenotype that was very similar to the phenotype observed in the conditional knockouts shown in figure 2. Kidneys from mice administered doxycycline for 1 months had numerous tubular microcysts accompanied by a dense interstitial inflammation (figure 6(ii)B), which on higher magnification revealed shrunken glomeruli, with collapsed capillary walls and proliferation of epithelial cells that filled the urinary space (figure 6(ii)D). Thus, these results demonstrate that miRNAs are required to the maintenance of normal podocyte function and suggest that primary changes in specific miRNAs may contribute to disease.

In order to begin to identify candidate miRNAs that are critical for normal podocyte function, glomeruli were isolated by laser capture microscopy from Drosha$^{fl/fl}$;podocin-rtTA$^{tg/+}$; tetO-Cre$^{Tg/+}$ and Drosha$^{fl/+}$;podocin-rtTA$^{tg/+}$; tetO-Cre$^{Tg/+}$ 4 weeks following administration of doxycycline, and miRNAexpression was quantitated by Taqman low density micro arrays. These experiments identified 10 miRNAs that were consistently undetectable in mice in which Drosha was conditionally inducibly deleted in podocytes when compared with heterozygote animals (Figure 7).

Discussion

In this study we demonstrate that conditional deletion of Drosha in podocytes results in CG that is similar to 3 previous reports that studied mice with a conditional deletion of Dicer in podocytes.[24–26] While both Drosha and Dicer have been shown to function in series to generate a mature miRNA, both RNAase molecules have distinct functions. For example, it is now appreciated that Dicer also plays a role in processing pseudogene-derived dsRNAs into siRNAs in mammals.[27, 28, 37] Thus, it remained a possibility that the kidney phenotype in podocyte-specific Dicer knockouts was contributed by other functions of Dicer. Moreover, whether Dicer and by extension miRNAs are critical for function of fully differentiated mature podocytes was not addressed in these previous studies. Our findings reported when taken together both reinforce the importance for miRNAs in podocyte homeostasis and/or development, and demonstrates for the first time that mature podocytes require the continued expression of miRNAs for normal function.

Conditional deletion of Drosha in podocytes resulted in a kidney lesion with many of the hallmarks of CG.[38, 39] The earliest phenotype observed was foot process effacement on electron microscopy, which was accompanied by proteinuria. As the disease progressed, podocytes underwent dedifferentiation leading to the loss of expression of podocyte specific genes such as podocin, nephrin, synaptopodin and WT1. These changes were accompanied by glomerular tuft collapse, wrinkling of the basement membrane, and pseudocrescent formation, which ultimately led to renal failure and death in most mice by 6 weeks of age.

One of the hallmarks of CG is the accumulation of proliferating epithelial cells in Bowman's space.[38–41] This is in contrast to other podocyte diseases, such as focal segmental glomerular sclerosis (FSGS), which is associated with podocyte loss, and lack the proliferative component seen in CG. Consistent with the histological features of CG, *NPHS2-Cre; Drosha$^{fl/fl}$* mice also had marked epithelial cell proliferation in glomeruli as assessed by Ki-67 staining. One of the controversies has been whether the proliferating cells

in CG derive from dedifferentiated podocytes or the parietal epithelial cells (PEC) that line the urinary space.[42–46] Lineage-tracing experiments have provided support for the contribution of both cell types to the proliferating epithelial cells in Bowman's space, depending upon the model studied.[42, 43, 46, 47] Our finding that about 80% of the proliferating epithelial cells in *NPHS2-Cre; Drosha*$^{fl/fl}$ mice express the podocyte-specific marker nestin as well as desmin, suggests that the majority of cells in the urinary space that form pseudocrescents are podocytes in origin. This would be in agreement with the podocyte lineage-tracing experiments by Moeller et al. [45, 47]as well as studies by Thorner et al.[35] While the mechanism whereby podocyte injury predisposes to the formation of pseudocrescents derived predominantly from podocytes or parietal epithelial cells is still unknown, these findings raise the possibility that specific miRNAs in podocytes are critical to maintaining podocytes in a nonproliferative differentiated state. Thus, loss of specific miRNAs in some diseases that affect podocytes may be one of the factors that determine whether podocytes are able to undergo a phenotypic switch that allows them to contribute to pseudocrescent formation. This is consistent with known functions of miRNAs in other cell types. For example, it has been shown that miR-1 and miR-206 play critical roles in skeletal muscle differentiation by maintaining skeletal muscle in a quiescent state.[48, 49]

Epithelial cells derived from *NPHS2-Cre; Drosha*$^{fl/fl}$ mice express the intermediate filament desmin and αSMA. While desmin has been shown to be upregulated in damaged podocytes,[33, 34] our finding that desmin positive cells in *NPHS2-Cre; Drosha*$^{fl/fl}$ mice also express SMA, raises the possibility that these cells are undergoing a type 2 epithelial-mesenchymal transition (EMT),[50, 51] which contributes to glomerular fibrosis and renal failure. EMT is not an easy diagnosis to make in vivo as there currently is not a single specific change that marks this transition. Rather, it has now been proposed that analyzing changes in expression of a number of different markers, including cytoskelatal proteins, transcription factors, matrix proteins, cell surface receptors, and miRNAs are required to identify cells undergoing EMT.[50] So far, we have been unable to demonstrate expression of some other markers of EMT in these cells, such as snail and beta catenin. Nevertheless, the finding that previous studies have shown that podocytes may undergo EMT in vitro,[52] together with the finding that miRNAs regulate EMT in other cells,[53] suggests that future studies should address whether podocytes undergo EMT in vivo and, if so, whether miRNAs play a role in this process.

One of the new findings reported here is that inducible conditional deletion of Drosha in podocytes at 2 months of age led to a rapid CG with proteinuria detected after less than 2 weeks after being treated with doxycycline. This finding not only supports the critical role for miRNAs in the maintenance of normal function of the mature podocyte, but strongly supports the idea that primary changes in specific miRNAs in the various podocytopathies may directly mediate disease. Identifying these miRNAs and the genes they regulate will likely provide new insight into disease pathogenesis as well as novel therapeutic targets.

Methods

Mice

Podocyte-specific *Drosha* knockouts were generated by crossing *NPHS2-Cre* transgenic mice with mice containing a conditional allele of *Drosha*^{fl}. *Drosha*^{fl} contains two lox P sites that flank exon 9.[29] *NPHS2-Cre* has been shown to be activated specifically in podocytes using a Rosa26 reporter.[54] Mice were genotyped by PCR using tail DNA and primer pairs previously reported. [29, 54]

Podocyte-specific *Dicer* knockouts were generated using a similar strategy by crossing *NPHS2-Cre* transgenic mice with mice containing a conditional allele of *Dicer*^{fl}. *Dicer*^{fl}

mice have been previously reported and were a generous gift of M. McManus, UCSF.[30] Both *Drosha* and *Dicer* mice were backcrossed onto a C57BL/6 genetic background for 8 generations.

Histology—Mice were perfused with 4% paraformaldehyde (PFA) through the heart. Kidneys were then either embedded in OCT and snap frozen or fixed in 4% paraformaldehyde overnight followed by embedding in paraffin. Periodic acid-Schiff (PAS) staining was performed on 4 mm paraffin sections according to a standard protocol.[55]

Immunohistochemistry—Paraffin sections were immunostained using the antibodies described below and detected using the avidin-biotin immunoperoxidase technique (Vector Laboratories) or fluorescent antibodies as previously described.[41]

Antibodies—The antibodies used in these studies were: anti-smooth muscle actin (clone 1A4, Sigma), anti-synaptopodin (clone G1D4, Progen Biotechnik), anti-WT-1 (Santa Cruz Biotechnology, Santa Cruz, Ca), anti-desmin (clone D33, Dako, Carpenteria, Ca), anti-nestin (clone 2Q178, Santa Cruz Biotechnology, Santa Cruz, Ca), and anti-ZO1, Alexa Fluor 594 goat anti-rabbit IgG and Alexa Fluor 488 goat anti-mouse Ig (Invitrogen, Carlsbad, CA). Anti-podocin anti-nephrin antibodies are rabbit polyclonal antibodies that have been previously described.

Electron Microscopy—Kidney cortex was sliced into 1 mm^3 cubes, fixed in 2% glutaraldehyde solution, and then processed using a standard protocol.

Proteinuria and blood urea nitrogen (BUN) determination—Urine was collected and protein concentration was determined using The Bradford protein assay (Bio-Rad),[56] as well as by the separation of unconcentrated urine by SDS-PAGE followed by staining with coumassie. Blood urea nitrogen concentration on serum was determined using the QuantichromTM urea assay kit (BioAssay Systems, Ca).

Podocyte Proliferation—4 mm paraffin sections were stained with an antibody to Ki-67 (Dako, Carpenteria, Ca). A proliferative index was determined by counting the number of glomeruli with Ki-67 positive cells in the urinary space per total number of glomeruli as described in Table 4.

Apoptosis—TUNEL staining was performed with the DeadEnd™ Fluorometric TUNEL System as per the manufacturer's directions (Promega, Madison, WI). The number of TUNEL-positive cells per 100 glomeruli was counted in sections from three control and three mutantkidneys from each group.

Generation of conditional inducible deletion of Drosha in podocytes—$Drosha^{fl/fl}$ mice described above were crossed to transgenic mice expressing both the reverse tetracycline transactivator (rtTA) under the control of the podocyte-specific podocin promoter NPHS2 (podocin-rrTA) and the cre recombinase driven by a minimal CMV promoter downstream of tet operon sequences. Cre was then induced in 8 week old mice ($Drosha^{fl/fl}$;podocin-$rtTA^{tg/+}$; tetO-$Cre^{Tg/+}$) by supplementing doxycyline (4 mg/ml) to the drinking water for 1–2 weeks as previously described.[36] Animals were sacrificed 4 weeks after the administration of doxycycline and kidneys were analyzed as described above. $Drosha^{fl/fl}$;podocin-$rtTA^{tg/+}$; tetO-$Cre^{Tg/+}$ not administered doxycycline served as controls.

Laser capture microdissection and RNA Extraction—To isolate glomeruli, laser capture microdissection was performed with PixCell II (Arcturus Bioscience). 4-μm frozen

kidney sections were dehydrated in graded ethanol solutions, stained with hematoxyin and eosin, placed in xylene and air dried. Laser capture was performed under direct microscopic visualization by melting of selected regions onto a thermoplastic film mounted on optically transparent LCM caps (Arcturus Engineering, Mountain View, CA). The PixCell II LCM System (Arcturus Engineering) was set to the following parameters: 7.5-μm laser spot size, 60-mW power, 15.0-ms duration. The thermoplastic film containing the microdissected glomeruli was incubated with 50 uL extraction buffer and total RNA was extracted as per the manufacturer's instructions (PicoPure RNA Isolation Ki, KIT0204, Arcturus). To eliminate potential genomic DNA contamination, RNA samples were treated with RNAse free DNase. RNA concentration was measured by nanodrop and quality assessed by bioanalyzer.

Quantitative real time PCR profiling on TLDA arrays—Rodent TaqMan® Low Density Array (TLDA) plate A and B version 2 microfluidics cards (Applied Biosystems) were used to assess the miRNA profiles. The contents of the TLDA A card comprised a total of 343 miRNAs. Experimental samples from 3 independent mice were profiled by ABI Prism 7900HT Sequence Detection System and miRNA levels were normalized to the average of U6 and U87 controls contained on the plate. The array data were analyzed by SDS software (Applied Biosystems) using the RQ = 2.0−ΔΔCT method, visualized in Agilent Genespring GX11 software where they were filtered on flag calls, then analyzed for reproducibly modulated profiles.

Verification of Drosha deletion in podocytes—Glomeruli were isolated from 2 month old *NPHS2-Cre; Drosha*$^{fl/fl}$ mice that were either untreated or treated with doxycyline for 2 weeks. Glomeruli were then isolated using Dynabeads as previously described [57], yielding a populatiton of > 90% glomeruli. PCR was then performed on glomerular DNA using primers flanking the loxP sites (Drosha-F GCAGAAAGTCTCCCACTCCT, Drosha-R-KO AACAACTGGGGCTGAAGAGA), which detect deletion of exon 9 in the Drosha gene.

Acknowledgments

We thank Dr Michael T McManus for the *Dicer*$^{f/f}$ mice, and Dr. Susan Quaggin for the podocin-rtTA; tetO-Cre transgenic mice. We thank the NYU Genome Technology Center supported in part by NIH/NCI grant P30 CA016087-30 for expert assistance with TLDA array profiling of miRNA expression. EYS is supported by grants R01GM084195 and R01AI052459. OZ is supported in part by grant 1UL1RR029893 from the National Center for Research Resources, National Institutes of Health.

References

1. Bartel DP. MicroRNAs: genomics, biogenesis, mechanism, and function. Cell. 2004; 116:281–297. [PubMed: 14744438]
2. Rana TM. Illuminating the silence: understanding the structure and function of small RNAs. Nat Rev Mol Cell Biol. 2007; 8:23–36. [PubMed: 17183358]
3. Filipowicz W, Bhattacharyya SN, Sonenberg N. Mechanisms of post-transcriptional regulation by microRNAs: are the answers in sight? Nat Rev Genet. 2008; 9:102–114. [PubMed: 18197166]
4. Eulalio A, Huntzinger E, Izaurralde E. Getting to the root of miRNA-mediated gene silencing. Cell. 2008; 132:9–14. [PubMed: 18191211]
5. Lee Y, Ahn C, Han J, et al. The nuclear RNase III Drosha initiates microRNA processing. Nature. 2003; 425:415–419. [PubMed: 14508493]
6. Lee Y, Kim M, Han J, et al. MicroRNA genes are transcribed by RNA polymerase II. EMBO J. 2004; 23:4051–4060. [PubMed: 15372072]
7. Han J, Lee Y, Yeom KH, et al. Molecular basis for the recognition of primary microRNAs by the Drosha-DGCR8 complex. Cell. 2006; 125:887–901. [PubMed: 16751099]

8. Kim VN. MicroRNA biogenesis: coordinated cropping and dicing. Nat Rev Mol Cell Biol. 2005; 6:376–385. [PubMed: 15852042]
9. Chendrimada TP, Gregory RI, Kumaraswamy E, et al. TRBP recruits the Dicer complex to Ago2 for microRNA processing and gene silencing. Nature. 2005; 436:740–744. [PubMed: 15973356]
10. Gregory RI, Chendrimada TP, Cooch N, et al. Human RISC couples microRNA biogenesis and posttranscriptional gene silencing. Cell. 2005; 123:631–640. [PubMed: 16271387]
11. Bartel DP. MicroRNAs: target recognition and regulatory functions. Cell. 2009; 136:215–233. [PubMed: 19167326]
12. Erson AE, Petty EM. MicroRNAs in development and disease. Clin Genet. 2008; 74:296–306. [PubMed: 18713256]
13. Stefani G, Slack FJ. Small non-coding RNAs in animal development. Nat Rev Mol Cell Biol. 2008; 9:219–230. [PubMed: 18270516]
14. Garzon R, Calin GA, Croce CM. MicroRNAs in Cancer. Annu Rev Med. 2009; 60:167–179. [PubMed: 19630570]
15. Kato M, Arce L, Natarajan R. MicroRNAs and their role in progressive kidney diseases. Clin J Am Soc Nephrol. 2009; 4:1255–1266. [PubMed: 19581401]
16. Li JY, Yong TY, Michael MZ, et al. Review: The role of microRNAs in kidney disease. Nephrology (Carlton). 2010; 15:599–608. [PubMed: 20883280]
17. Kato M, Putta S, Wang M, et al. TGF-beta activates Akt kinase through a microRNA-dependent amplifying circuit targeting PTEN. Nat Cell Biol. 2009; 11:881–889. [PubMed: 19543271]
18. Wei Q, Bhatt K, He HZ, et al. Targeted deletion of Dicer from proximal tubules protects against renal ischemia-reperfusion injury. J Am Soc Nephrol. 2010; 21:756–761. [PubMed: 20360310]
19. Wang Q, Wang Y, Minto AW, et al. MicroRNA-377 is up-regulated and can lead to increased fibronectin production in diabetic nephropathy. FASEB J. 2008; 22:4126–4135. [PubMed: 18716028]
20. Krupa A, Jenkins R, Luo DD, et al. Loss of MicroRNA-192 promotes fibrogenesis in diabetic nephropathy. J Am Soc Nephrol. 21:438–447. [PubMed: 20056746]
21. Pandey P, Brors B, Srivastava PK, et al. Microarray-based approach identifies microRNAs and their target functional patterns in polycystic kidney disease. BMC Genomics. 2008; 9:624. [PubMed: 19102782]
22. Lee SO, Masyuk T, Splinter P, et al. MicroRNA15a modulates expression of the cell-cycle regulator Cdc25A and affects hepatic cystogenesis in a rat model of polycystic kidney disease. J Clin Invest. 2008; 118:3714–3724. [PubMed: 18949056]
23. Anglicheau D, Sharma VK, Ding R, et al. MicroRNA expression profiles predictive of human renal allograft status. Proc Natl Acad Sci U S A. 2009; 106:5330–5335. [PubMed: 19289845]
24. Shi S, Yu L, Chiu C, et al. Podocyte-selective deletion of dicer induces proteinuria and glomerulosclerosis. J Am Soc Nephrol. 2008; 19:2159–2169. [PubMed: 18776119]
25. Ho J, Ng KH, Rosen S, et al. Podocyte-specific loss of functional microRNAs leads to rapid glomerular and tubular injury. J Am Soc Nephrol. 2008; 19:2069–2075. [PubMed: 18832437]
26. Harvey SJ, Jarad G, Cunningham J, et al. Podocyte-specific deletion of dicer alters cytoskeletal dynamics and causes glomerular disease. J Am Soc Nephrol. 2008; 19:2150–2158. [PubMed: 18776121]
27. Tam OH, Aravin AA, Stein P, et al. Pseudogene-derived small interfering RNAs regulate gene expression in mouse oocytes. Nature. 2008; 453:534–538. [PubMed: 18404147]
28. Watanabe T, Totoki Y, Toyoda A, et al. Endogenous siRNAs from naturally formed dsRNAs regulate transcripts in mouse oocytes. Nature. 2008; 453:539–543. [PubMed: 18404146]
29. Chong MM, Rasmussen JP, Rudensky AY, et al. The RNAseIII enzyme Drosha is critical in T cells for preventing lethal inflammatory disease. J Exp Med. 2008; 205:2005–2017. [PubMed: 18725527]
30. Harfe BD, McManus MT, Mansfield JH, et al. The RNaseIII enzyme Dicer is required for morphogenesis but not patterning of the vertebrate limb. Proc Natl Acad Sci U S A. 2005; 102:10898–10903. [PubMed: 16040801]

31. DePianto D, Coulombe PA. Intermediate filaments and tissue repair. Exp Cell Res. 2004; 301:68–76. [PubMed: 15501447]
32. Floege J, Alpers CE, Sage EH, et al. Markers of complement-dependent and complement-independent glomerular visceral epithelial cell injury in vivo. Expression of antiadhesive proteins and cytoskeletal changes. Lab Invest. 1992; 67:486–497. [PubMed: 1279269]
33. Floege J, Hackmann B, Kliem V, et al. Age-related glomerulosclerosis and interstitial fibrosis in Milan normotensive rats: a podocyte disease. Kidney Int. 1997; 51:230–243. [PubMed: 8995738]
34. Hoshi S, Shu Y, Yoshida F, et al. Podocyte injury promotes progressive nephropathy in zucker diabetic fatty rats. Lab Invest. 2002; 82:25–35. [PubMed: 11796823]
35. Thorner PS, Ho M, Eremina V, et al. Podocytes contribute to the formation of glomerular crescents. J Am Soc Nephrol. 2008; 19:495–502. [PubMed: 18199804]
36. Jones N, New LA, Fortino MA, et al. Nck proteins maintain the adult glomerular filtration barrier. J Am Soc Nephrol. 2009; 20:1533–1543. [PubMed: 19443634]
37. Suh N, Baehner L, Moltzahn F, et al. MicroRNA function is globally suppressed in mouse oocytes and early embryos. Curr Biol. 2010; 20:271–277. [PubMed: 20116247]
38. Albaqumi M, Barisoni L. Current views on collapsing glomerulopathy. J Am Soc Nephrol. 2008; 19:1276–1281. [PubMed: 18287560]
39. D'Agati VD. Podocyte injury in focal segmental glomerulosclerosis: Lessons from animal models (a play in five acts). Kidney Int. 2008; 73:399–406. [PubMed: 17989648]
40. Barisoni L, Schnaper HW, Kopp JB. Advances in the biology and genetics of the podocytopathies: implications for diagnosis and therapy. Arch Pathol Lab Med. 2009; 133:201–216. [PubMed: 19195964]
41. Barisoni L, Mokrzycki M, Sablay L, et al. Podocyte cell cycle regulation and proliferation in collapsing glomerulopathies. Kidney Int. 2000; 58:137–143. [PubMed: 10886558]
42. Appel D, Kershaw DB, Smeets B, et al. Recruitment of podocytes from glomerular parietal epithelial cells. J Am Soc Nephrol. 2009; 20:333–343. [PubMed: 19092119]
43. Asano T, Niimura F, Pastan I, et al. Permanent genetic tagging of podocytes: fate of injured podocytes in a mouse model of glomerular sclerosis. J Am Soc Nephrol. 2005; 16:2257–2262. [PubMed: 15987751]
44. Dijkman HB, Weening JJ, Smeets B, et al. Proliferating cells in HIV and pamidronate-associated collapsing focal segmental glomerulosclerosis are parietal epithelial cells. Kidney Int. 2006; 70:338–344. [PubMed: 16761013]
45. Moeller MJ, Soofi A, Hartmann I, et al. Podocytes populate cellular crescents in a murine model of inflammatory glomerulonephritis. J Am Soc Nephrol. 2004; 15:61–67. [PubMed: 14694158]
46. Suzuki T, Matsusaka T, Nakayama M, et al. Genetic podocyte lineage reveals progressive podocytopenia with parietal cell hyperplasia in a murine model of cellular/collapsing focal segmental glomerulosclerosis. Am J Pathol. 2009; 174:1675–1682. [PubMed: 19359523]
47. Smeets B, Uhlig S, Fuss A, et al. Tracing the origin of glomerular extracapillary lesions from parietal epithelial cells. J Am Soc Nephrol. 2009; 20:2604–2615. [PubMed: 19917779]
48. Kim HK, Lee YS, Sivaprasad U, et al. Muscle-specific microRNA miR-206 promotes muscle differentiation. J Cell Biol. 2006; 174:677–687. [PubMed: 16923828]
49. Chen JF, Callis TE, Wang DZ. microRNAs and muscle disorders. J Cell Sci. 2009; 122:13–20. [PubMed: 19092056]
50. Zeisberg M, Neilson EG. Biomarkers for epithelial-mesenchymal transitions. J Clin Invest. 2009; 119:1429–1437. [PubMed: 19487819]
51. Kalluri R, Weinberg RA. The basics of epithelial-mesenchymal transition. J Clin Invest. 2009; 119:1420–1428. [PubMed: 19487818]
52. Li Y, Kang YS, Dai C, et al. Epithelial-to-mesenchymal transition is a potential pathway leading to podocyte dysfunction and proteinuria. Am J Pathol. 2008; 172:299–308. [PubMed: 18202193]
53. Korpal M, Kang Y. The emerging role of miR-200 family of microRNAs in epithelial-mesenchymal transition and cancer metastasis. RNA Biol. 2008; 5:115–119. [PubMed: 19182522]
54. Moeller MJ, Sanden SK, Soofi A, et al. Podocyte-specific expression of cre recombinase in transgenic mice. Genesis. 2003; 35:39–42. [PubMed: 12481297]

55. Barisoni L, Bruggeman LA, Mundel P, et al. HIV-1 induces renal epithelial dedifferentiation in a transgenic model of HIV-associated nephropathy. Kidney Int. 2000; 58:173–181. [PubMed: 10886562]

56. Bradford MM. A rapid and sensitive method for the quantitation of microgram quantities of protein utilizing the principle of protein-dye binding. Anal Biochem. 1976; 72:248–254. [PubMed: 942051]

57. Takemoto M, Asker N, Gerhardt H, et al. A new method for large scale isolation of kidney glomeruli from mice. Am J Pathol. 2002; 161:799–805. [PubMed: 12213707]

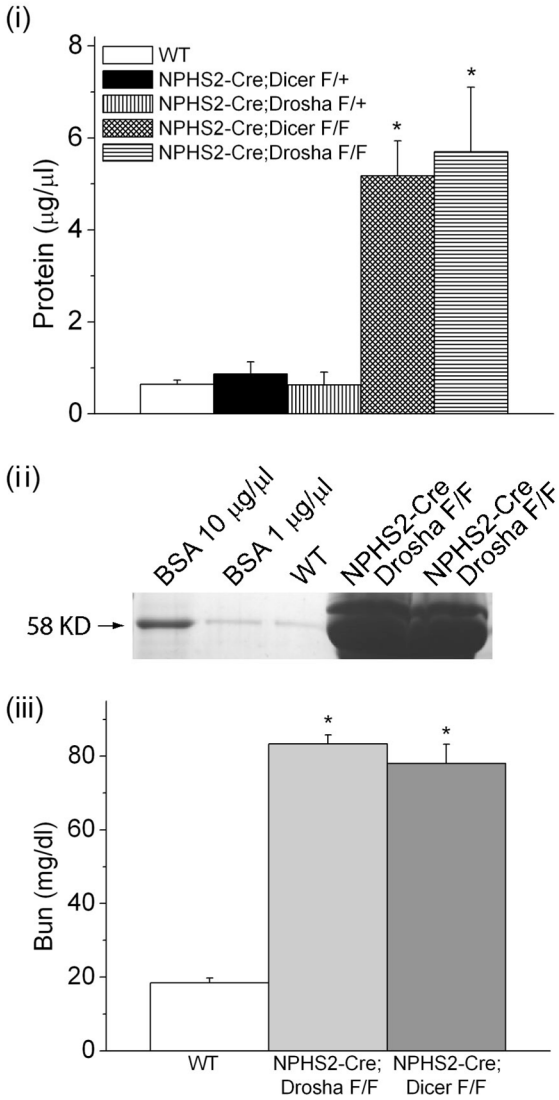

Figure 1. *NPHS2-Cre; Drosha$^{fl/fl}$* develop proteinuria and renal failure

(i) Protein concentration in urine obtained from WT (*NPHS2-Cre; Drosha$^{+/+}$*), heterozygous (*NPHS2-Cre; Drosha$^{fl/+}$*), and homozygous Drosha (*NPHS2-Cre; Drosha$^{fl/fl}$*) and Dicer (*NPHS2-Cre; Dicer$^{fl/fl}$*) mutants determined by Bradford assay (n=5 mice in each group). Differences in protein concentrations were statistically significant for homozygous Drosha and Dicer mice when compared with WT and homozygous animals (* P<0.05). (ii) 10 ul of urine from 4 week old WT and homozygous Drosha mutants were separated by SDS polyacrylamide gel electrophoreses (10%) followed by coumassie staining. Bovine serum albumin (BSA) was run as a control. (iii) Bun concentration was determined in 4 week old WT and homozygous Drosha and Dicer mutants (n= 5 mice in each group). Bun values were statistically significant in homozygous Drosha and Dicer mice when compared to WT mice (* P<0.05).

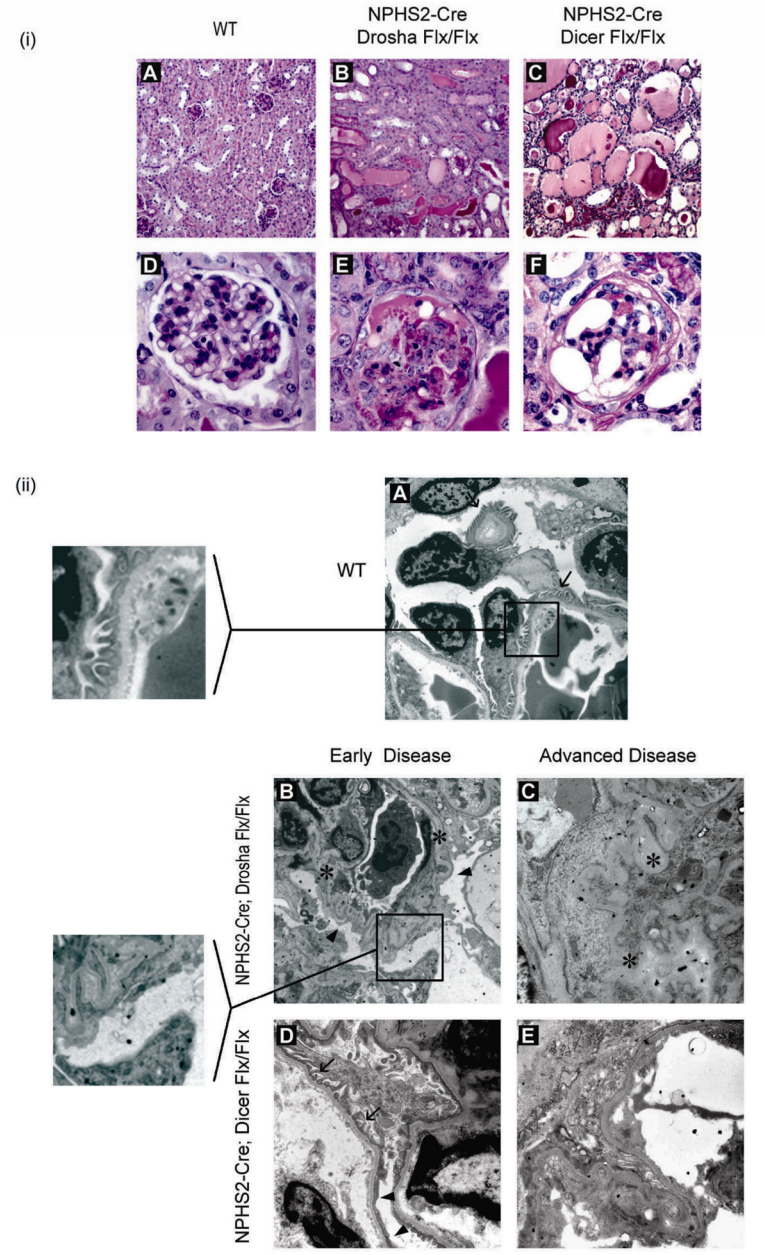

Figure 2. *NPHS2-Cre; Drosha*$^{fl/fl}$ develop collapsing glomerulopathy with focal glomerulosclerosis with pseudocrescent and microcystic dilatation of tubules

(i) Histologic examination (PAS stain) of kidneys from WT (*NPHS2-Cre; Drosha*$^{+/+}$) and homozygous Drosha (*NPHS2-Cre; Drosha*$^{fl/fl}$) and Dicer (*NPHS2-Cre; Dicer*$^{fl/fl}$) mutants at 4–5 weeks of age. Upper panel, 20X magnification (A–C); lower panel, 40X magnification (D–F). (ii) Electron microscopy of kidneys from WT (A) or homozygous Drosha and Dicer mutants at 2 weeks (early disease-B, D) or 4–5 weeks (advanced disease-C,E) of age. Arrows indicate normal podocyte foot processes. Arrowheads indicate effaced podocyte foot processes. Asterisks indicate collapsed glomerular basement membrane. Insert in panel A shows normal podocyte foot processes. Insert in Panel B shows effaced podocyte foot processes.

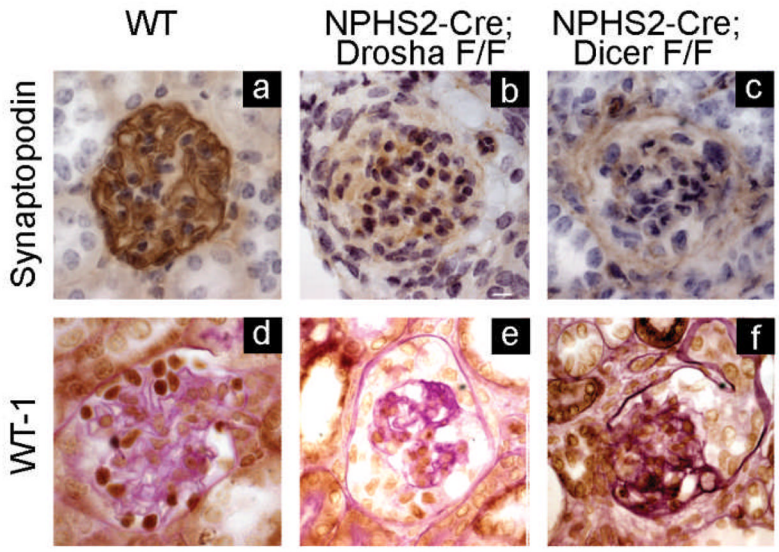

Figure 3. Podocytes from Drosha and Dicer mutants have decreased expression of synaptopodin and WT-1

Immunohistochemistry of histologic sections from 4–5 week old WT, Drosha, and Dicer mutants immunostained with antibodies to synaptopodin and WT-1. Podocyte expression of synaptopodin and WT are decreased in both Drosha and Dicer mutants.

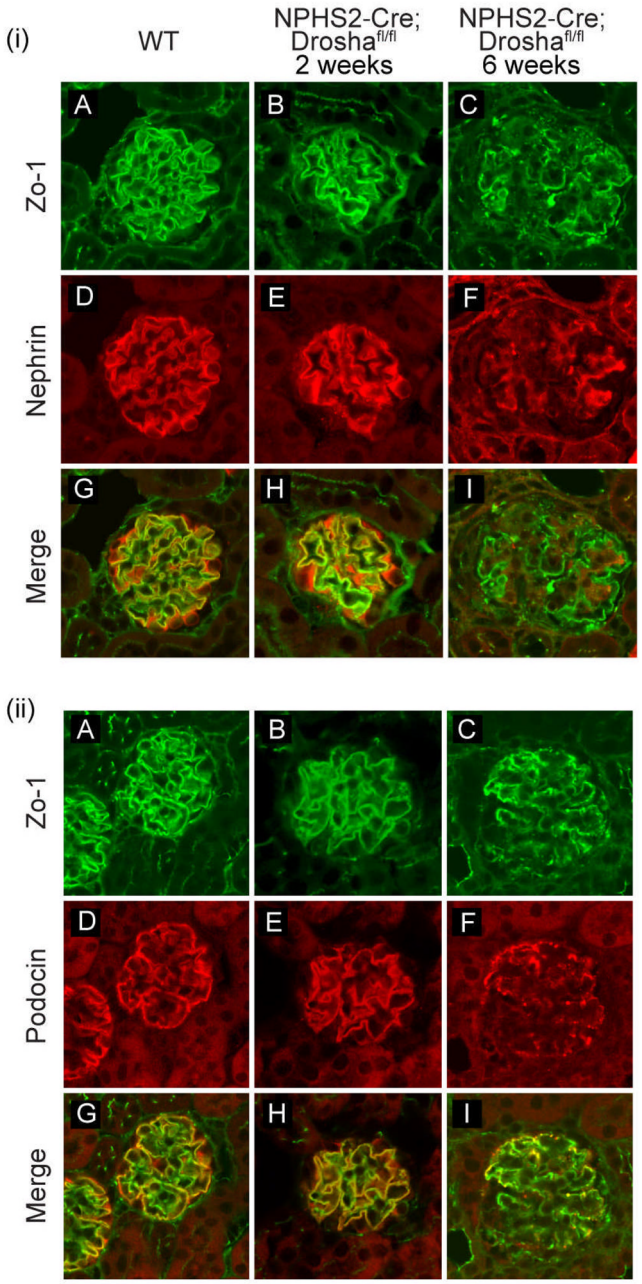

Figure 4. Expression of podocin and nephrin in WT and Drosha mutants

Immunofluorescence of histologic sections from WT and Drosha mutants at 2 and 6 weeks of age stained with antibodies to (i) nephrin (D–F) and (ii) podocin (D–F). Sections were also stained with anit-ZO1 to mark adherent junctions on podocytes (i) A–C and (ii) A–C.

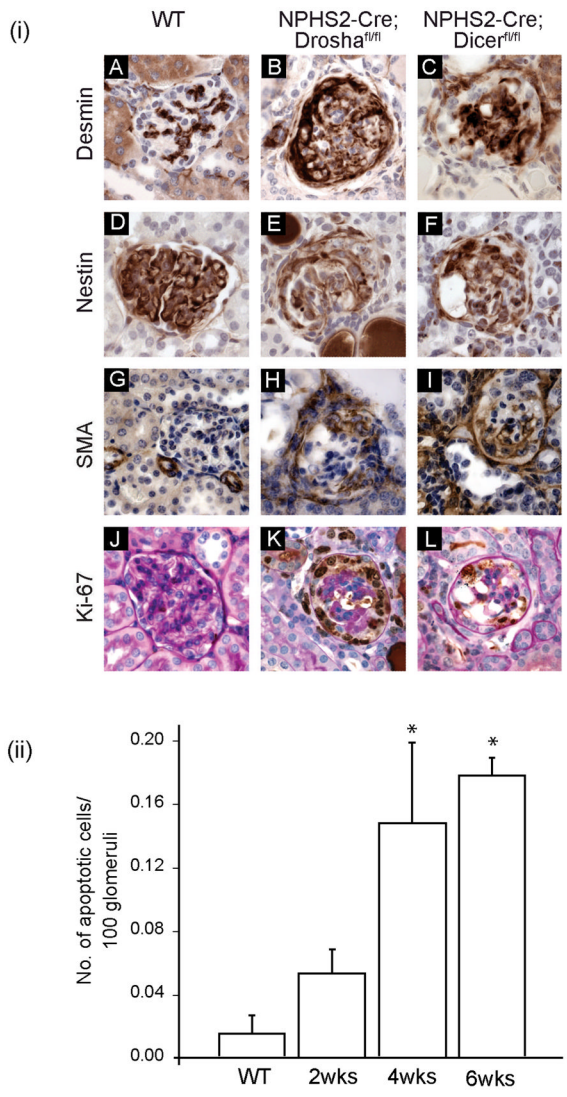

Figure 5. Pseudocrescents stain positive for desmin, nestin, SMA, and Ki-67

(i) Immunohistochemistry of histological sections from 4–5 week old WT (*NPHS2-Cre; Drosha*$^{+/+}$), homozygous Drosha (*NPHS2-Cre; Drosha*$^{fl/fl}$) and Dicer (*NPHS2-Cre; Dicer*$^{fl/fl}$) mutants immunostained with antibodies as indicated. (ii) *NPHS2-Cre; Drosha*$^{fl/fl}$ demonstrate increased apoptosis as CG becomes more advanced. Statistically significant for 4 and 6 week old *NPHS2-Cre; Drosha*$^{fl/fl}$ when compared to WT animals or 2 week old *NPHS2-Cre; Drosha*$^{fl/fl}$ (* $P<0.05$).

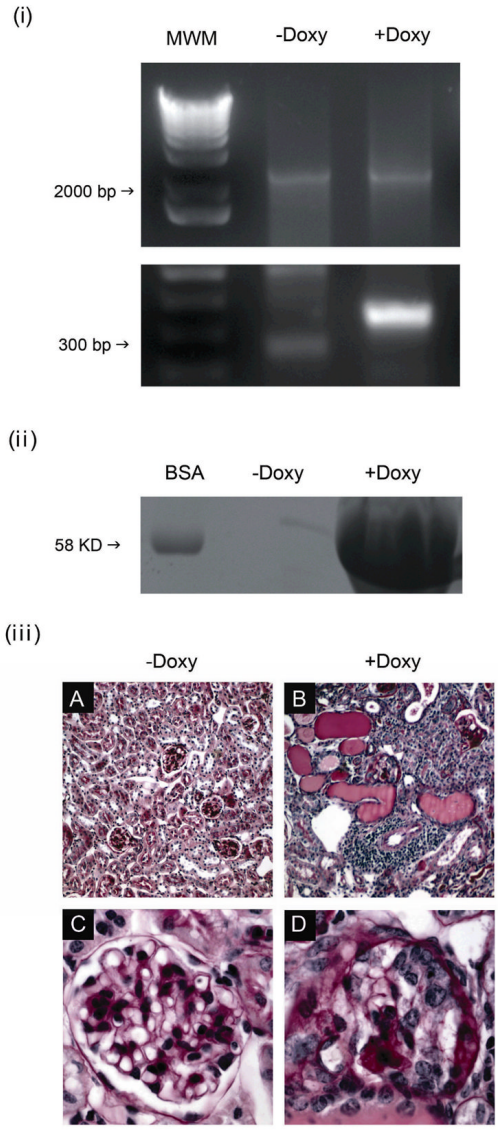

Figure 6. Conditional inducible deletion of Drosha in podocytes in 2 month old animals results in a collapsing glomerulopathy

(i) Glomeruli were isolated from Drosha$^{fl/fl}$;podocin-rtTA$^{tg/+}$; tetO-Cre$^{tg/+}$ mice that were either administered or not administered doxycycline and deletion of exon 9 was assessed by PCR using primers that flank the loxP site. Deletion of exon 9 results in a product of 334 base pairs, in contrast to the 2.5 Kb product in the wild type gene. 1kB plus Invitrogen was used as molecular weight marker (MWM) (ii) 10 ul of urine from Drosha$^{fl/fl}$;podocin-rtTA$^{tg/+}$; tetO-Cre$^{tg/+}$ mice that were administered or not administered doxycycline for 2–4 weeks were separated by SDS polyacrylamide gel electrophoreses (10%) followed by coumassie staining. Bovine serum albumin (BSA) was run as a control. (iii) Drosha$^{fl/fl}$;podocin-rtTA$^{tg/+}$; tetO-Cre$^{tg/+}$ mice were either administered, or not administered doxycycline at 2 months of age and kidneys were analyzed 1 month later. Shown are PAS stains of kidneys sections from (A,C) Dox-minus and (B,D) Dox-plus animals. Figure (A) shows normal glomeruli and unremarkable tubule-interstitum (20X). On higher magnification (C, 40X), glomeruli are normal in size and cellularity and mesangium is normally expanded. Glomerular basement membranes are also unremarkable. No

proliferation in the urinary space is noted. In contrast, animals fed doxycycline (B, 20X) had numerous tubular microcysts and a dense interstitial inflammation, which on higher magnification (D, 40X) revealed shrunken glomeruli, with collapsed capillary walls and proliferation of epithelial cells that filled the urinary space.

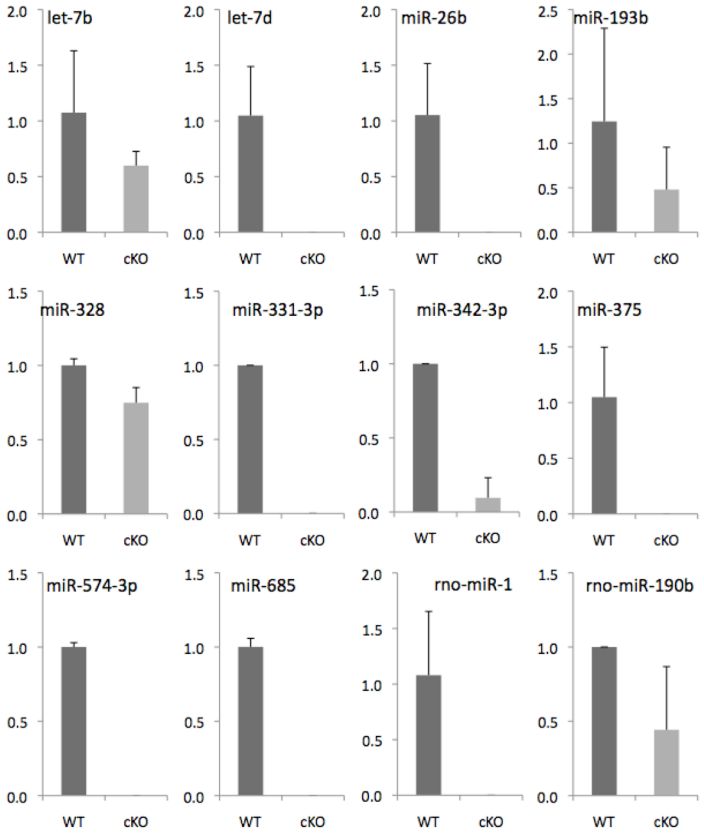

Figure 7. miRNA expression in glomeruli from Doxycycline-minus and Doxycyline-plus animals

2 month old Drosha$^{fl/fl}$;podocin-rtTA$^{tg/+}$; tetO-Cre$^{Tg/+}$ mice were either administered or not administered doxycycline for 2 weeks and glomeruli were isolated by laser capture microdissection as described in Materials and Methods. RNA was then reversed transcribed and miRNA expression was quantitated using Taqman Low Density Microarrays (Applied Biosystems). Shown are 10 miRNAs that were consistently markedly downregulated in doxycycline treated animals from 3 independent experiments.

Table 1

Histologic analysis between 4–6 weeks of age

Genotype/Phenotype	% Segm sclerosis	% Segm collapse	% Global sclerosis	%global collapse	Tub. Microcysts
NPHS2-Cre; Drosha$^{+/+}$	0	0	0	0	0
NPHS2-Cre; Drosha$^{fl/fl}$	14.5	14.8	12.7	29.9	3+
NPHS2-Cre; Dicer$^{fl/fl}$	9.3	14.8	26.3	22.9	3+

Segmental sclerosis: segmental solidification of the glomerular tuft with adhesion to the Bowman's capsule

Segmental collapse: segmental wrinkling and folding of the glomerular basement membranes with hypertrophy and hyperplasia of overlying podocytes.

Global sclerosis: global solidification of tuft

Global collapse: global wrinkling and folding of the glomerular basement membranes with hypertrophy and hyperplasia of overlying podocytes filling the urinary space.

Tubular Microcysts: defined as dilated tubules containing hyaline casts. The amount of microcysts is calculated on a semiquantitative scale from 0–3+ (0 = no cysts; +/− = < 10 cysts total at 40X; 1+ = 1–3 cysts in at least 5 fields at 40X; 2+ = 4–10 cysts in at least 5 fields at 40X; 3+ = >11 cysts in at least 5 fields at 40X)

Table 2

Characterization of renal disease in NPHS2-Cre; Drosha$^{fl/fl}$ and NPHS2-Cre; Dicer$^{fl/fl}$ mice

	NPHS2-Cre; Drosha$^{+/+}$	NPHS2-Cre; Drosha$^{fl/fl}$	NPHS2-Cre; Dicer$^{fl/fl}$
Proteinuria	–	+++	+++
Glomerular sclerosis & collapse*	0%	71.9%	73.4%
Tubular microcysts*	0	3+	3+
Podocyte phenotype**	Normal	Abnormal	Abnormal
Foot process effacement	0%	100%	100%
Primary Processes	Present	Absent	Absent

Note:

* See Table 1 legend for details;

** details of podocyte phenotype in regard to podocin, nephrin, synaptopodin, WT-1, Ki-67, SMA, desmin, nestin are discussed in the text and shown in Table 2.

Table 3

Podocyte phenotype – immunohistochemical analysis

	NPHS2-Cre; Drosha$^{+/+}$	NPHS2-Cre; Drosha$^{fl/fl}$	NPHS2-Cre; Dicer$^{fl/fl}$
Synaptopodin	+	−	−
WT-1	+	−	−
Nestin	+	+	+
SMA	−	+	+
Desmin	−	+	+
Ki-67	−	+	+

Note: '+' positive staining; '−' negative staining

Table 4

Proliferative index of epithelial cell in urinary space

	Glomeruli with Ki-67 + cells in urinary space per total number of collapsed glomeruli (range)
NPHS2-Cre; Drosha$^{+/+}$	0
NPHS2-Cre; Drosha$^{fl/fl}$ (2weeks)	0
NPHS2-Cre; Drosha$^{fl/fl}$ (4–6 weeks)	0.656 (0.261–0.753)